

**Ministry of Higher Education
and Scientific Research
University of Diyala
College of Engineering**



STRENGTH AND BEHAVIOR OF REINFORCED CONCRETE RING DEEP BEAMS

**A Thesis Submitted to Council of College of Engineering,
University of Diyala in Partial Fulfillment of the
Requirements for the Degree of Master of Science in Civil
Engineering**

By

**Abdullah Abdulrahman Talal
(B.Sc. in Civil Engineering, 2017)**

Supervised by:

Prof. Khattab Saleem Abdul-Razzaq, (Ph. D.)

March, 2021 A.D.

IRAQ

Shaban, 1442 A.H.

بِسْمِ اللّٰهِ الرَّحْمٰنِ الرَّحِیْمِ
وَقُلِ اَعْمَلُوا فِی سَبِیْلِ اللّٰهِ عَمَلًا وَّرِسْوَلَهُ
وَالْمُؤْمِنُوْنَ وَسْتُرْدُوْنَ اِلٰی عَالَمِ الْغَیْبِ
وَالشَّهَادَةِ فِی نَبِیِّكُمْ بِمَا كُنْتُمْ تَعْمَلُوْنَ

صدق الله العظيم

التوبة-105

DEDICATION

All praise to Allah, today we leave the days' tiredness and the errand summing up between the covers of this humble work, ..

To the utmost knowledge lighthouse, to our greatest and most honored Prophet Mohamed (Peace Be Upon Him) ...

To whom he strives to bless comfort and welfare and never stints what he owns to push me in the success way, who taught me to promote life stairs wisely and patiently, to my dearest father...

To the spring that never stops giving, to my mother who weaves my happiness with strings from her merciful heart...

To who always helps and supports me... my brother Huthaifa...

Abdullah Abdulrahman Talal

2021

ACKNOWLEDGEMENTS

*In the name of Allah, the most gracious, the most merciful, before anything, I thank **ALLAH** who enabled me to achieve this research.*

*First, I wish to express my sincere gratitude and appreciation to the supervisor; **Prof. Khattab S. Abdul-Razzaq (Ph. D.)** for his supervisions, precious advices, technical guidance, continuous encouragements, and remarkable patience in reviewing my thesis and stop me pause forearm to a person's, I'm really indebted to him.*

*My thanks go as well to **all friends** who have donate advice and did not complain of frequent questions especially **Asala A Dawood, Wissam H Khalil and Ali M Jalil.***

*Great thanks to the staff of **Structural Engineering Laboratory** in addition to my teachers in the **Department of Civil Engineering** for their cooperation and help.*

*I would like to express my thanks, appreciation and gratitude to **my family** for their support and patience that helped me in achieving this study, which is the fruit of our entire family.*

Abdullah Abdulrahman Talal

2021

Strength and Behavior of Reinforced Concrete Ring Deep Beams

By

Abdullah Abdulrahman Talal

Supervisor:

Prof. Dr. Khattab Saleem Abdul-Razzaq

ABSTRACT

The main goal of this study is to investigate the behavior of reinforced concrete ring deep beams based on the STM of ACI 318M-14. This research includes casting and testing program for eight reinforced concrete ring deep beam specimens divided into four groups. The sectional width of all specimens is 100mm with a diameter of 1000mm c/c. All specimens are subjected to single concentrated load at mid of each span and supported on three supports except one of them. The variables that have been considered are as follows: secondary reinforcement, main reinforcement, height of ring deep beam, and number of supports. The first group comprises removing horizontal secondary reinforcement, removing vertical secondary reinforcement, and removing both of them together. The second group comprises decreasing quantity of main reinforcement by about 61% and 100%. The third group comprises reducing the height from 350 mm to 300 mm, i.e., 14%. The fourth group had increased in the number of supports from 3 to 4.

The experimental ultimate capacity, load-deflection response, deflection at first crack, crack type and propagation, in addition to crack characteristics were all investigated and discussed. Besides to failure conditions, strain values in steel bars and average strain values in concrete surfaces are also investigated.

The experimental results show that the load-midspan deflection responses obtained for the tested specimens are roughly linear for the majority of the loading process, then bend slightly, except when vertical shear reinforcement is omitted or no secondary reinforcement is provided, in addition to the case of no main reinforcement. This illustrates the most common shear deformation behavior, which leads to brittle failure. The experimental results also show the efficacy of the ACI 318 STM, although it is conservative by 37-41%. The lateral displacement at the load application point is also measured. Until the appearance of the first crack, the dependence of the torsional moments and lateral displacement is nearly linear. After cracking, the lateral displacement significantly increased. Load capacity decreased by about 12.5%, 38.5%, and 55%, when removing horizontal secondary reinforcement, removing vertical secondary reinforcement, and removing both of them together respectively. While the midspan deflection decreased by about 15% when removing horizontal secondary reinforcement, removing vertical secondary reinforcement and removing both of them together led to increase deflection by 0.5%, and 32.8% respectively. The load capacity and midspan deflection were not affected when the main reinforcement ratio decreased by about 61%, because the failure was a strut shear failure. As for when the main reinforcement was completely removed, the failure shifted from the strut to the tie, and the load capacity and midspan deflection decreased by about 36% and 23.5%, respectively. Reducing the height from 350 mm to 300 mm, i.e., 14%, led to decrease the load capacity by about 15%, while the midspan deflection increased by about 32.8%. The increase in the number of supports from 3 to 4 led to increase load capacity by about 63%, while midspan deflection decreased by about 48%.

Table of Contents

TABLE OF CONTENTS

Subject	Page No.
Dedication	iii
Acknowledgement	iv
Abstract	v
Table of Contents	vii
List of Figures	x
List of Plates	xiii
List of Tables	xiv
List of Symbols and Terminology	xv
CHAPTER ONE INTRODUCTION	
1.1 General	1
1.2 Modeling with Struts and Ties	1
1.2.1 Regions of Discontinuities in Reinforced Concrete Members	2
1.2.2 Elements of Strut and Tie Model	4
1.2.2.1 Struts	4
1.2.2.2 Ties	5
1.2.2.3 Nodes	6
1.3 Horizontally curved Beam	7
1.4 Analysis of horizontally curved Beam	9
1.4.1 Statically Hand Calculation Analysis	9
1.4.2 Finite Element Analysis Using ETABS-2018	13
1.5 Reinforcement Limitations	14
1.5.1 Secondary Reinforcement Limitations	14
1.5.2 Main Reinforcement Limitations	14
1.5.3 Concrete Cover Limitations	14
1.6 Advantages of using the deep ring beams	14
1.7 Objectives of The study	15
1.8 Thesis Layout	16
CHAPTER TWO LITERATURE REVIEW	
2.1 Introduction	17
2.2 Strut and Tie Modeling	17
2.3 Experimental Investigations	22
2.4 Numerical Analysis of Horizontally Curved and Ring Beams	26
2.5 Concluding Remarks	33
CHAPTER THREE EXPERIMENTAL WORK	
3.1 Introduction	36
3.2 Experimental Programme	36
3.2.1 R.16.4.4.350.3	39
3.2.2 R.16.4.0.350.3	39
3.2.3 R.16.0.4.350.3	40
3.2.4 R.16.0.0.350.3	41
3.2.5 R.10.4.4.350.3	41

Table of Contents

3.2.6 R.0.4.4.350.3	42
3.2.7 R.16.4.4.300.3	43
3.2.8 R.16.4.4.350.4	43
3.3 Construction Materials	44
3.3.1 Cement	44
3.3.2 Fine Aggregate	45
3.3.3 Coarse Aggregate	46
3.3.4 Steel Reinforcement	47
3.4 Normal Concrete Mix Design	48
3.5 Mixing Procedures	48
3.6 Slump Test for Fresh Concrete	49
3.7 Molds	50
3.8 Casting and Curing	50
3.9 Control Specimens	53
3.9.1 Compressive Strength Test	53
3.9.2 Splitting Tensile Strength Test	54
3.9.3 Modulus of Rupture Test	54
3.10 Test Measurements and Instrumentation	55
3.10.1 Deflection Measurements	55
3.10.2 Crack Width	56
3.10.3 Steel and Concrete Strain Measurement	57
3.10.3.1 Location of Strain Gauges	57
3.10.3.2 TDS-530 Data Logger	60
3.11 Testing Procedure	60
CHAPTER FOUR RESULTS AND DISCUSSION	
4.1 General	63
4.2 Properties of the Mixed Concrete	63
4.2.1 Fresh Properties	63
4.2.2 Hardened Concrete Properties	64
4.3 Behavior of Reinforced Concrete Ring Deep Beams	64
4.3.1. Group A	66
4.3.1.1 R.16.4.4.350.3	67
4.3.1.2 R.16.4.0.350.3	68
4.3.1.3 R.16.0.4.350.3	69
4.3.1.4 R.16.0.0.350.3	70
4.3.2. Group B	71
4.3.2.1 R.10.4.4.350.3	71
4.3.2.2 R.0.4.4.350.3	72
4.3.3. Group C	73
4.3.3.1 R.16.4.4.300.3	73
4.3.4. Group D	74
4.3.4.1 R.16.4.4.350.4	75
4.4 Load-deflection Response & Load-lateral displacement relationship	76
4.4.1 Specimens of Group A	84
4.4.2 Specimens of Group B	85
4.4.3 Specimens of Group C	85
4.4.4 Specimens of Group D	86

Table of Contents

4.5 Crack Width Measurements	86
4.5.1 Flexural Cracks	88
4.5.2 Diagonal Cracks	88
4.6 Strain Values Reading	93
4.6.1 Average Strains of Concrete Surface	93
4.6.2 Steel Reinforcement Strain Values	98
4.7 Comparisons between the Results of Experimental Work and STM of ACI 318M-14	103
4.8 Summary	104
4.8.1 The Effect of secondary reinforcement	104
4.8.1.1 Load Ultimate Capacity	104
4.8.1.2 Central deflection	105
4.8.1.3 Lateral Displacement	105
4.8.1.4 Strain values	106
4.8.2 Effect of Height	106
4.8.2.1 Ultimate load capacity	106
4.8.2.2 Deflection	106
4.8.2.3 Lateral displacement	107
4.8.2.4 Strain values	107
4.8.3 Effect of decreasing the number of supports	107
4.8.3.1 Ultimate load capacity	107
4.8.3.2 Deflection	107
4.8.3.3 Lateral displacement	108
4.8.3.4 Strain values	108
4.8.4 Effect of main reinforcement	108
4.8.4.1 Ultimate load capacity	108
4.8.4.2 Deflection	108
4.8.4.3 Lateral displacement	109
4.8.4.4 Strain values	109
4.9 Strut and Tie Modelling Validation	109
CHAPTER FIVE NUMERICAL ANALYSIS	
5.1 General	111
5.2 Conclusions	111
5.3 Recommendations for Future Work	114
REFERENCES	115
APPENDIX A	A-1
APPENDIX B	B-1
APPENDIX C	C-1

LIST OF FIGURES

Figure No.	Figure Title	Page No.
1-1	Strut and tie model, prismatic strut type	2
1-2	Typical D regions, (ACI 318-14, Chapter 23)	3
1-3	Bottle and Fan types of struts	5
1-4	Nodal and extended nodal zones	7
1-5	Maximum moments and shear locations in horizontally curved beam segment	8
1-6	single convention (Yee–Chit Wong, 1970)	9
1-7	Variation of fixed end bending moment coefficients with span angle for horizontally curved beams loaded with concentrated load. (Yee–Chit Wong, 1970)	10
1-8	Variation of fixed end torsional moment coefficients with span angle for horizontally curved beams loaded with concentrated load. (Yee–Chit Wong, 1970)	11
1-9	Variation of maximum span moment coefficients with span angle for horizontally curved beams loaded with concentrated load. (Yee–Chit Wong, 1970)	11
1-10	Variation of deflection coefficients with span angle for horizontally curved beams loaded with concentrated load. (Yee–Chit Wong, 1970)	12
1-11	Rectangular section of a deep beam	13
1-12	Ring beams	15
2-1	Beam details (mm), (Yang and Ashour, 2011)	18
2-2	Details of tested continuous deep beams, (Beshara, et al., 2012)	20
2-3	Geometry of Test Specimens of Badawy et al (Badawy, 1977)	24
2-4	Beams after failure, (M. Abul Mansur and B. Vijaya Rangan, 1981)	26
2-5	Fixed ends horizontally curved deep beam resting on an elastic foundation under uniform distributed load (q), Al-Azzawi and Shaker (2011)	29
3-1	Experimental program scheme	37
3-2	Specimen R.16.4.4.350.3	39
3-3	Specimen R.16.4.0.350.3	40
3-4	Specimen R.16.0.4.350.3	40
3-5	Specimen R.16.0.0.350.3	41
3-6	Specimen R.10.4.4.350.3	42
3-7	Specimen R.0.4.4.350.3	42
3-8	Specimen R.16.4.4.300.3	43
3-9	Specimen R.16.4.4.350.4	44
3-10	The slump measurement test	50
3-11	LVDTs locations for three and four supports specimens	55
3-12	Positions of strain gauges on concrete surface	58
3-13	Positions of strain gauges on steel reinforcement	59
4-1	1 st diagonal cracking loads for the specimens of Group A	67
4-2	1 st cracking loads for the specimens of Group B	71
4-3	1 st diagonal cracking loads for the specimens of Group C	73
4-4	1 st diagonal cracking loads for the specimens of Group D	75

List of Figures

4-5	Load-deflection response for Specimen R.16.4.4.350.3, (Reference)	76
4-6	Load-deflection response for Specimen R.16.4.0.350.3, group A	77
4-7	Load-deflection response for Specimen R.16.0.4.350.3, group A	77
4-8	Load-deflection response for Specimen R.16.0.0.350.3, group A	78
4-9	Load-deflection response for Specimen R.10.4.4.350.3, group B	78
4-10	Load-deflection response for Specimen R.0.4.4.350.3, group B	79
4-11	Load-deflection response for Specimen R.16.4.4.300.3, group C	79
4-12	Load-deflection response for Specimen R.16.4.4.350.4, group D	80
4-13	Load-lateral displacement response for Specimen R.16.4.4.350.3, Reference	81
4-14	Load- lateral displacement response for Specimen R.16.4.0.350.3, group A	81
4-15	Load- lateral displacement response for Specimen R.16.0.4.350.3, group A	81
4-16	Load- lateral displacement response for Specimen R.16.0.0.350.3, group A	82
4-17	Load- lateral displacement response for Specimen R.10.4.4.350.3, group B	82
4-18	Load- lateral displacement response for Specimen R.0.4.4.350.3, group B	82
4-19	Load- lateral displacement response for Specimen R.16.4.4.300.3, group C	83
4-20	Load- lateral displacement response for Specimen R.16.4.4.350.4, group D	83
4-21	Group A load-deflection response	84
4-22	Group B load-deflection response	85
4-23	Group C load-deflection response	86
4-24	Group D load-deflection response	86
4-25	Load-1 st flex. crack width for group B	88
4-26	Load-1 st diag. crack width for group A	89
4-27	Load-1 st diag. crack width for group B	90
4-28	Load-1 st diag. crack width for group C	91
4-29	Load-1 st diag. crack width for group D	91
4-30	Diagonal cracks comparison of all specimens	92
4-31	Applied load versus concrete average strain values for specimen R.16.4.4.350.3 (Reference)	94
4-32	Applied load versus concrete average strain values for specimen R.16.4.0.350.3 (Group A)	94
4-33	Applied load versus concrete average strain values for specimen R.16.0.4.350.3 (Group A)	95
4-34	Applied load versus concrete average strain values for specimen R.16.0.0.350.3 (Group A)	95
4-35	Applied load versus concrete average strain values for specimen R.10.4.4.350.3 (Group B)	96
4-36	Applied load versus concrete average strain values for specimen R.0.4.4.350.3 (Group B)	96
4-37	Applied load versus concrete average strain values for specimen R.16.4.4.300.3 (Group C)	97
4-38	Applied load versus concrete average strain values for specimen R.16.4.4.350.4 (Group D)	97

List of Figures

4-39	Applied load versus concrete average strain for specimen R.16.4.4.350.3 (Reference)	99
4-40	Applied load versus reinforcing steel strain values for specimen R.16.4.0.350.3 (Group A)	99
4-41	Applied load versus reinforcing steel strain values for specimen R.16.0.4.350.3 (Group A)	100
4-42	Applied load versus reinforcing steel strain values for specimen R.16.0.0.350.3 (Group A)	100
4-43	Applied load versus reinforcing steel strain values for specimen R.10.4.4.350.3 (Group B)	101
4-44	Applied load versus reinforcing steel strain values for specimen R.0.4.4.350.3 (Group B)	101
4-45	Applied load versus reinforcing steel strain values for specimen R.16.4.4.300.3 (Group C)	102
4-46	Applied load versus reinforcing steel strain values for specimen R.16.4.4.350.4 (Group D)	102
4-47	Comparisons between P_{STM} and P in group A	104
4-48	Comparisons between P_{STM} and P in group B	104
4-49	Comparisons between P_{STM} and P in group C	104
4-50	Comparisons between P_{STM} and P in group D	104
A-1	Strut and Tie model for the reference R.16.4.4.350.3	A-2
A-2	Specimen R.16.4.4.350.3	A-2
A-3	Reinforcement crossing strut	A-4
A-4	Reinforcement crossing strut	A-4
A-5	Forces of nodal zone	A-4
C-1	Applied torque at first crack	C-3
C-2	Applied concentrated load at first crack $P_{cr-diag}$	C-3
C-3	Finite element modeling for typical ring beam	C-4
D-1	Load-lateral displacement response for Specimen R.16.4.4.350.3, Reference	D-1
D-2	Load- lateral displacement response for Specimen R.16.4.0.350.3, group A	D-1
D-3	Load- lateral displacement response for Specimen R.16.0.4.350.3, group A	D-2
D-4	Load- lateral displacement response for Specimen R.16.0.0.350.3, group A	D-2
D-5	Load- lateral displacement response for Specimen R.10.4.4.350.3, group B	D-3
D-6	Load- lateral displacement response for Specimen R.0.4.4.350.3, group B	D-3
D-7	Load- lateral displacement response for Specimen R.16.4.4.300.3, group C	D-4
D-8	Load- lateral displacement response for Specimen R.16.4.4.350.4, group D	D-4

LIST OF PLATES

Plate No.	Plate Title	Page No.
3-1	Graded natural sand of Al-Sodur	45
3-2	Crushed gravel with 10 mm maximum size of particles	46
3-3	Steel bar testing machine	47
3-4	Slump test cone	50
3-5	Slump test measuring	50
3-6	Steel mold used for casting specimens	50
3-7	Steel reinforcing cages for all tested specimens	51
3-8	Compressive strength test f'_c , splitting tensile strength test f_{ct} and modulus of rupture test f_r	52
3-9	Casting of the specimens	52
3-10	Specimen during the curing time	53
3-11	White painting of the ring specimens	53
3-12	Concrete compressive strength test	53
3-13	Splitting tensile strength test	54
3-14	Modulus of rupture test	55
3-15	LVDTs used to measure central deflection and lateral displacement	56
3-16	Micro-crack meter device	56
3-17	Strain gauges type	57
3-18	Strain gauges indicator used in the present research work	60
3-19	Universal testing machine used to test the specimens of three supports	61
3-20	Load distributor	61
3-21	Universal testing machine used to test the specimen with four supports	62
4-1	Fresh concrete slump test	63
4-2	Specimen R.16.4.4.350.3 after testing	68
4-3	Specimen R.16.4.0.350.3 after testing	69
4-4	Specimen R.16.0.4.350.3 after testing	70
4-5	Specimen R.16.0.0.350.3 after testing	71
4-6	Specimen R.10.4.4.350.3 after testing	72
4-7	Specimen R.0.4.4.350.3 after testing	73
4-8	Specimen R.16.4.4.300.3 after testing	74
4-9	Specimen R.16.4.4.350.4 after testing	76
B	Installation of the electrical strain gauges and the used instruments	B-2

LIST OF TABLES

Table No.	Table title	Page No.
2-1	Specimens results, (Yang and Ashour, 2011)	19
2-2	Dimensions and steel reinforcing details, (Khatab, et al., 2016)	22
2-3	Effect of loading type (Talal, et al., 2021)	31
2-4	Effect of dimensions (Talal, et al., 2021)	31
2-5	The effect of the number of supports (Talal, et al., 2021)	31
3-1	Reinforcement details of all specimens	38
3-2	Physical properties of cement	44
3-3	Chemical composition and main compounds of cement	45
3-4	Fine aggregate grading	46
3-5	Physical properties of fine aggregate	46
3-6	Grading of coarse aggregate	47
3-7	Physical properties of coarse aggregate	47
3-8	Mechanical properties of steel bars reinforcement	48
3-9	Mix proportions of concrete	48
4-1	Slump test results of fresh concrete	64
4-2	Hardened concrete properties of the specimens	65
4-3	Experimental results for all tested specimens	66
4-4	Experimental crack characteristics	92
4-5	Values of experimental cracking loads vs. the cracking loads that obtained from strain diagrams	98

LIST OF SYMBOLS AND TERMINOLOGY

SYMBOLS

a	Shear span measured from support to load c/c, mm
A_h	Area of secondary horizontal reinforcement, mm ²
A_v	Area of secondary vertical reinforcement, mm ²
b	Width of cross section of ring deep beam, mm
d	Effective depth of beam, distance from extreme compression fiber to centroid of longitudinal tension reinforcement, mm
D	Diameter of ring deep beam specimen c/c, mm
E_c	Modulus of elasticity of concrete, MPa
E_s	Modulus of elasticity of steel reinforcement, MPa
f'_c	150mm×300mm Cylinder compressive strength of concrete, MPa
f_{ce}	Effective compressive strength of the concrete in a strut or a nodal zone, MPa
f_{ct}	Indirect tensile strength (splitting tensile strength), MPa
f_{cu}	Cube compressive strength of concrete
f_r	Modulus of rupture, MPa
f_y	Yield stress of main reinforcement (MPa)
f_{yh}	Yield stress of secondary vertical reinforcement, MPa
f_{yv}	Yield stress of secondary horizontal reinforcement, MPa
F_n	Capacity of STM members, kN
h	Total depth of ring deep beam, mm
j_d	Moment arm, mm
L_b	Length of load bearing block, mm
P	Failure load of ring deep beam, kN
P_{c-code}	ACI Code nominal concrete strength, kN
P_{c-exp}	Experimental concrete strength, kN
$P_{cr-diag}$	First diagonal cracking load, kN
$P_{cr-flex}$	First flexural cracking load, kN
P_n	Nominal applied load, kN
P_{s-code}	ACI Code nominal steel strength, kN
P_{s-exp}	Experimental steel strength, kN
P_{STM}	Theoretical load according to chapter 23, ACI 318M-14 Strut and Tie method, kN
S_h	Spacing of secondary horizontal reinforcement, mm
S_v	Spacing of secondary vertical reinforcement, mm
σ_{vB}	Ultimate stress of horizontal face of node, MPa
V_n	Nominal strength, kN
\emptyset_{main}	Diameter of bar for main reinforcement, mm
\emptyset_{st}	Diameter of bar for shear reinforcement, mm
w_{sb}	Width of strut at support nodal zone, mm
w_{st}	Width of strut at load nodal zone, mm
w_t	Width of anchor tie, mm
α_1, α_2	Inclination angle of reinforcement to the axis of the ring deep beam, degree
β_n	Nodal zone coefficient
β_s	Factor to account for the cracking effect and confining reinforcement on the effective compressive strength of the concrete in a strut
Δ	Displacement corresponding to the ultimate of ring deep beam, mm
$\Delta_{cr-diag}$	Displacement corresponding to the 1st diagonal crack load, mm

List of Symbols and Terminology

$\Delta_{cr-flex}$	Displacement corresponding to the 1st flexural crack load, mm
ϵ_{yield}	Strain at yield
θ	Angle of inclination of the diagonal compressive stress and the failure plane with the ring deep beam longitudinal axis in right side, degree
ρ	Main reinforcement ratio
ρ_h	Secondary horizontal reinforcement ratio
ρ_v	Secondary vertical reinforcement ratio
ϕ	Diameter of the bar, mm

TERMINOLOGY

a/d	Shear span to effective depth ratio
a/h	Shear span to overall depth ratio
ACI	American Concrete Institute
ASTM	American Society for Testing and Materials
BS	British Standard
c/c	Center to center clear span, mm
CCT	Compression- Compression- Tension
CSA	Canadian Standard Association
ALWC	All-Lightweight Concrete
SLWC	Sand-Lightweight Concrete
NWC	Normal Weight Concrete
ANSYS	Analysis System
HSC	High Strength Concrete
I.Q.S	Iraqi Standard Specification
JSCE	Japan Society of Civil Engineers
L_n/h	Clear span to overall depth ratio
RC	Reinforced Concrete
SCC	Self-Compacted Concrete
STM	Strut and Tie Model
NSC	Normal strength Concrete
NSM	Near Surface Mounted
Cc	Clear cover, mm

CHAPTER ONE

INTRODUCTION

1.1 General

It has been found advantageous to use horizontally curved deep beams or bow deep girders in building and bridge design. Recently, many architects and designers have become more interested in using them. Meantime, dome, silo, circular tank, offshore structures, and other structures use ring deep beams with a complete circular plane. Because of their high load resistance, industries have relied on ring deep beams (Al Qaicy, et al., 2014).

According to ACI 318M-14 Code, deep beams can be defined as: "Structural Members supported on one face and loaded on the opposite face so that struts-similar compression elements can expand between the supports and the loads, that states (1) or (2):

- 1) The clear span of the beam must not be more than four times the overall depth of the beam h .
- 2) Concentrated loads are those that occur within $2h$ of the support face."

In mathematical forms, shear span to the beam height ($a/h \leq 2$) should be taken into consideration for simple span and continuous deep beams.

1.2 Modeling with Struts and Ties

Strut and Tie Modeling is a way of analysis for reinforced concrete structures and reinforced concrete prestressed structures that decline complex states of stress in a structure to a gathering of simple stress paths. The stress paths cause uniaxial stresses in suggested truss members. Truss members in compression are named struts, whereas the force paths in tension are called ties. The junctions of ties - struts are called nodes as shown in

Figure (1-1). The combination of ties, struts and nodes is named a truss mechanism (Brown and Bayrak, 2006).

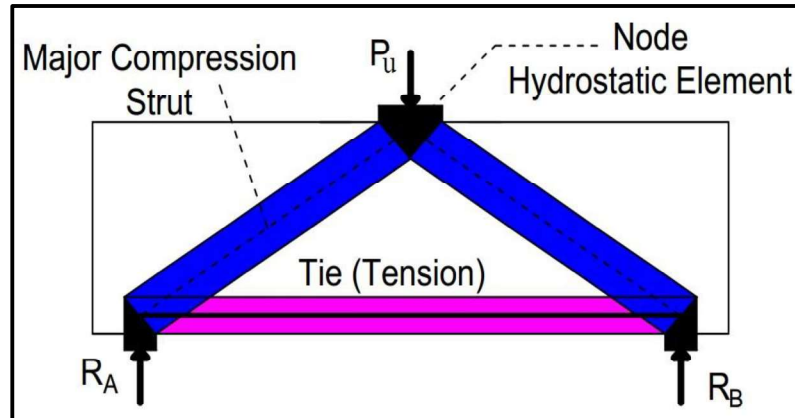


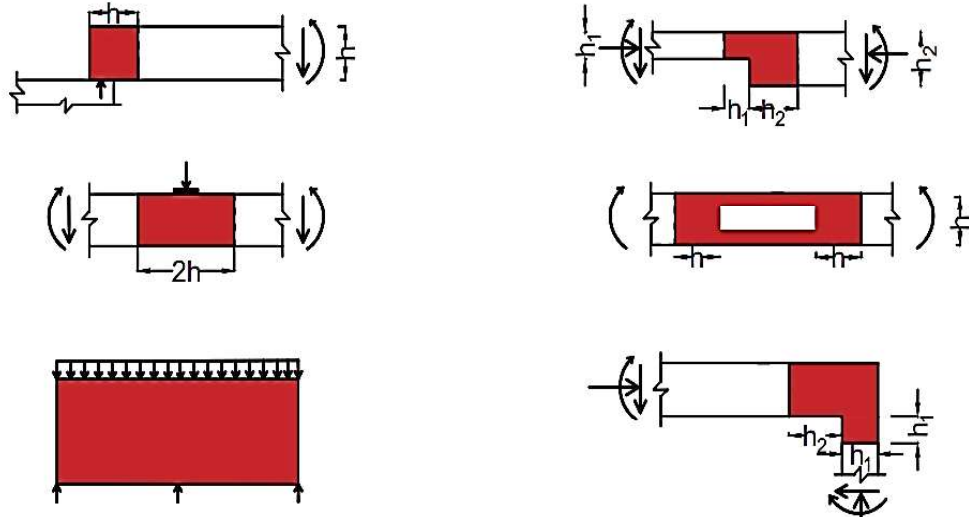
Figure (1-1): Strut and tie model, prismatic strut type

Strut and tie model overlooking kinematic constraints. Within the analysis stage, node equilibrium and overall equilibrium are considered. Empirical observation of ties, struts, and nodes is used to determine the constitutive relevance of these elements in order to set the yield conditions for them. As a result, strut and tie models follow the lower bound of plasticity theory, which states that only yield conditions and equilibrium must be persuaded (Brown and Bayrak, 2006). According to the lower bound of plasticity theory, if the load is large enough to allow the discovery of a stress distribution that is identical to stresses at the yield surface while maintaining external and internal equilibrium, the load will not cause the body to collapse (Nielsen, et al., 1978). More specifically, the capacity of a structure, as determined by a lower bound approach, will be at most equal to or less than the actual collapse load.

1.2.1 Regions of Discontinuities in Reinforced Concrete Members

When there is a change in the geometry of element in a structure or in a reaction or concentrated load as shown in Figure (1-2), an abrupt change in the distribution of stresses exists at that change. St. Venant's principle states that the stresses, because of bending and axial load, have linear distribution at a distance approximately equal to member height far from

the discontinuity. For this cause, discontinuities are considered to extend a distance h from the section where the change in geometry or load exists (ACI 318M-14 Code). Therefore, a structural element can be divided into the following regions:



Loading discontinuities

Geometric discontinuities

Figure (1-2): Typical D regions, (ACI 318-14, Chapter 23)

- **B Regions:** They function as parts of a member that can be used to solve the "plane section" assumptions of the conventional beam theory using a sectional design approach.
- **D Regions:** They're all the areas outside of the B zones where cross sectional planes don't stay plain after loading. When there are discontinuities or disturbances in the distribution of stress at parts of a structure member, D regions are commonly assumed (ACI 318M-14).

1.2.2 Elements of Strut and Tie Model

1.2.2.1 Struts

Struts are the elements that carry compressive stresses in strut-tie models. The geometry of a strut is determined by the applied load type. According to Nielsen et al. (1978), there are three types of struts:

- ***Prismatic Strut:*** the most basic type of struts. The cross-section of a prismatic strut is uniform throughout its length, as shown in Figure (1-1). When the compressive stresses are limited by the neutral axis, such a strut can exist in a beam. A prismatic strut is a representation of a beam's compressive stress block in a section of constant moment (Brown and Bayrak, 2006).
- ***Bottle-Shaped Strut:*** A bottle-shaped strut can be developed because the flow of compressive stresses is not restricted to a part of a structural element, as shown in Figure (1-3a). The load is applied to a small area in this case, and the stresses disperse as they flow through the member. The compressive stress changes direction as it divides, forming an angle with the strut's axis. A tensile force is formed to counteract the lateral component of the angled compression forces in order to maintain equilibrium.
- ***Compression Fan Strut:*** It is specialized due to the fact that it focuses care on such a small area. Stresses cause a radial flow from a large to a smaller area. When large uniform loads flow into a support, a compression fan is formed, as shown in Figure (1-3b). Because the forces are collinear and there are no tension components perpendicular to the fan zone, the developed tensile stresses have no value (Brown and Bayrak, 2006).

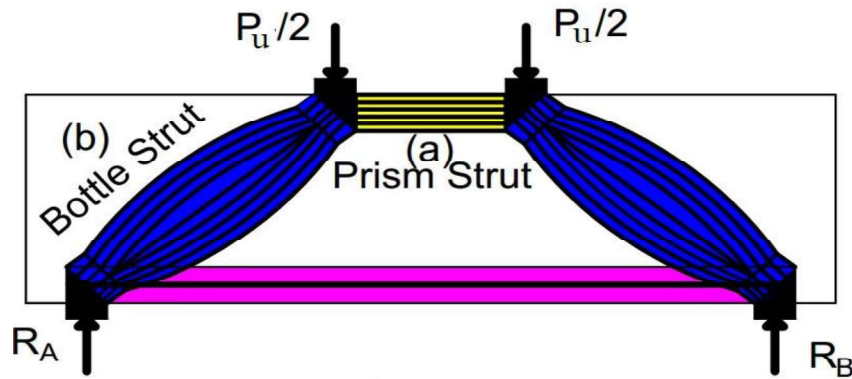


Figure (1-3a): Bottle Strut type

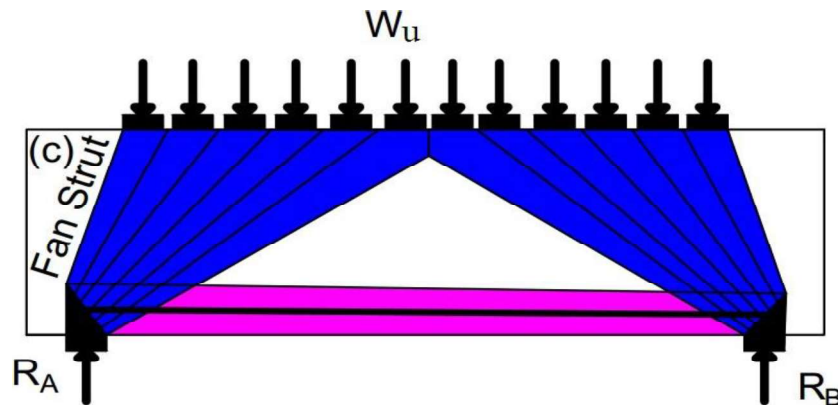


Figure (1-3b): Fan Strut type

Figure (1-3): Bottle and Fan types of struts

1.2.2.2 Ties

Ties are the elements that carry tension, mostly restricted to reinforcing bars. Therefore, the geometry of a tie is so simpler than the strut or the node. The tie is geometrically limited to elements that can carry high tensile forces, and the permitted force is primarily derived from the yield force.

Ties are made up of deformed rebar, prestressing rebar, or both, as well as a section of the enclosure concrete that is concentric with the tie axis. In the model, the enclosure concrete is almost never considered to be able to withstand axial force. While it reduces the elongation of the tie, also stiffens the tension in the tie, which is especially useful under service loads. It also specifies the area in which the ties and struts' forces are to be anchored.

1.2.2.3 Nodes

Nodes are the points of intersection of the struts axes, concentrated loads and ties, representing the joints of a strut and tie model (ACI 318M-14). The location at which forces are redirected within a strut and tie modeling is another way of defining a node. At least three forces on a given node of the model should work to preserve equilibrium. Based on the sign of the forces acting on them, nodes are listed as follows (Fu, 2001):

- C-C-C: is the node that resists three compressive forces.
- C-C-T: is the node that resists one tensile force and two compressive forces.
- C-T-T: is the node that resists two tensile forces and one compressive force.
- T-T-T: is the node that resists three tensile forces.
- T-T-C-C-C: is the node that resists two tensile forces and three compressive forces.

The amount of concrete presumed to transfer strut and tie forces through the node is referred to as the nodal region, Figure (1-4). The early strut and tie models used hydrostatic nodal zones, which were lately superseded by extended nodal zones. The hydrostatic term refers to the fact that the stresses in the plane are the same in all directions.

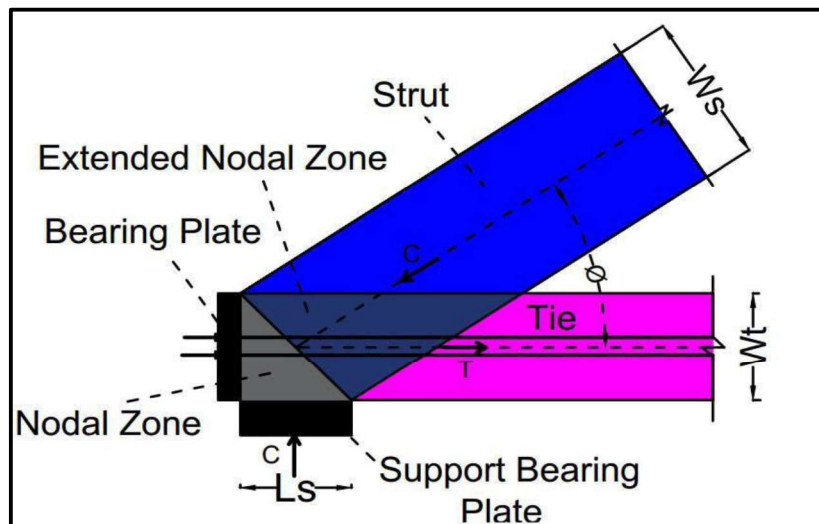


Figure (1-4): Nodal and extended nodal zones

1.3 Horizontally curved Beams

It is worth to mention that unlike a straight beam, the centroidal axis and the neutral axis of a horizontally curved beam are not coincident. In addition to that, from the neutral axis, the stresses do not vary linearly (Anderson, G., 1950). In a horizontally curved beam, torsional moments occur because the applied loads and the reactions do not lie over the main axis along the horizontally curved beam. These torsional moments become zero at the midspan between any two successive columns in case of circular beam that supported by equally spaced columns. Maximum torsional moments grow at sections closer to the supports in addition to the zones where the bending moment is zero, the maximum torque takes place at the points of contraflexure as shown in Figure (1-5). Moreover, positive maximum bending moments develop at sections in between the supports. Whereas the maximum negative bending moments occur at the support sections. About the shear forces, they are maximum at the support sections.

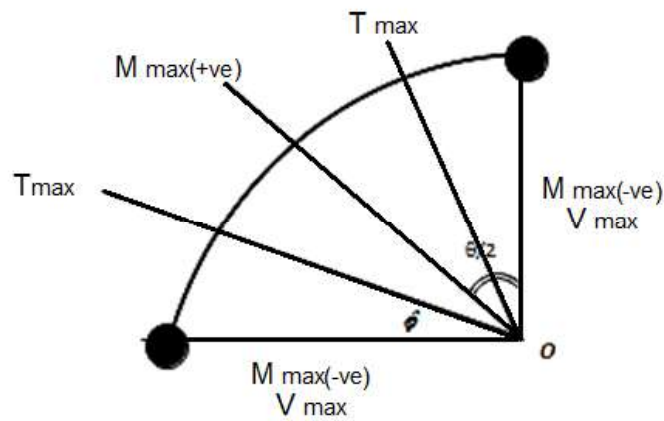


Figure (1-5): Maximum moments and shear locations in a horizontally curved beam segment

The difference in analysis and design between the straight beams and the beams horizontally curved in plane is fundamentally because of the presence of torsional moments caused by vertical load. Therefore, for such members, it is important to design both the twisting moment and the internal bending moment as well as the transverse shear. The capability of resisting torsional moments is expressed by torsional rigidity. That is defined as the torsional moment which, when applied to one free to rotate end, produces a unit angle of twist with respect to the other end assumed to be completely fixed (Andersen, P., 1953). The greater the torsional rigidity, the greater the resistance to the torque. The value of torsional rigidity depends on the shape of the section. It was found that the box sections have comparatively large values of torsional rigidity (Iyse, I., 1941) and, that is why are widely used in bridge design. However, the rectangular section is also commonly used. Horizontally curved beams, either made of steel or reinforced concrete, can be continuous or monolithic at both ends.

1.4 Analysis of Horizontally Curved Beams:

1.4.1 Statically Hand Calculation Analysis

Yee–Chit Wong, 1970, Oregon State University, 1970, presented a hand calculation analysis of ring beam that is adopted in the current study in addition to the finite element of ETABS software. Bending moments and torsional moments are expressed by moment vectors. Vertical force acting upward is represented by a solid circle O, Figure (1-6). An open circle O represents the vertical force acting downward. The bending moment is considered positive if it causes clockwise rotation around the radial axis when looking out from the center of the curvature. Torsional moments are considered positive, creating a clockwise rotation when looking in a counterclockwise direction along the tangent of the beam. Vertical force is considered positive when it acts upward. Figure (1-6) also shows the sign convention used in the current study analysis, while Figures (1-7) through (1-11) can be used to analyze horizontally circular ring beam manually.

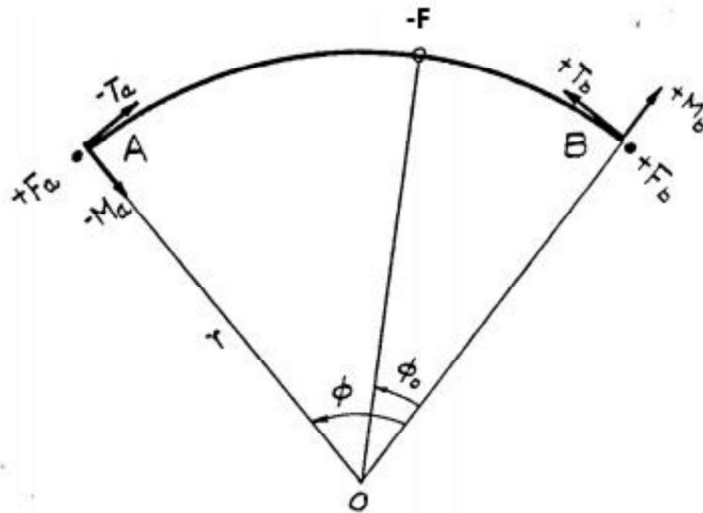


Figure (1-6): Singe convention (Yee–Chit Wong, 1970)

Based on the above, the forces and deflection are:

$$M_b = F \times r \times C_m \quad \text{-----} (1 - 1)$$

$$T_b = F \times r \times C_t \quad \text{-----} (1 - 2)$$

$$M_{\max} = F \times r \times C_{mm} \quad \text{-----} (1 - 3)$$

$$\Delta = \frac{Fr^3}{EI} C_d \quad \text{-----}(1-4)$$

where:

M_b	is	Negative moment
T_b	is	Torque
M_{max}	is	Positive moment
Δ	is	Deflection
F	is	Concentrated load at mid span
r	is	Radius
C_m, C_t, C_{mm}, C_d	are	Coefficients
E	is	Modulus of elasticity
I	is	Moment of inertia

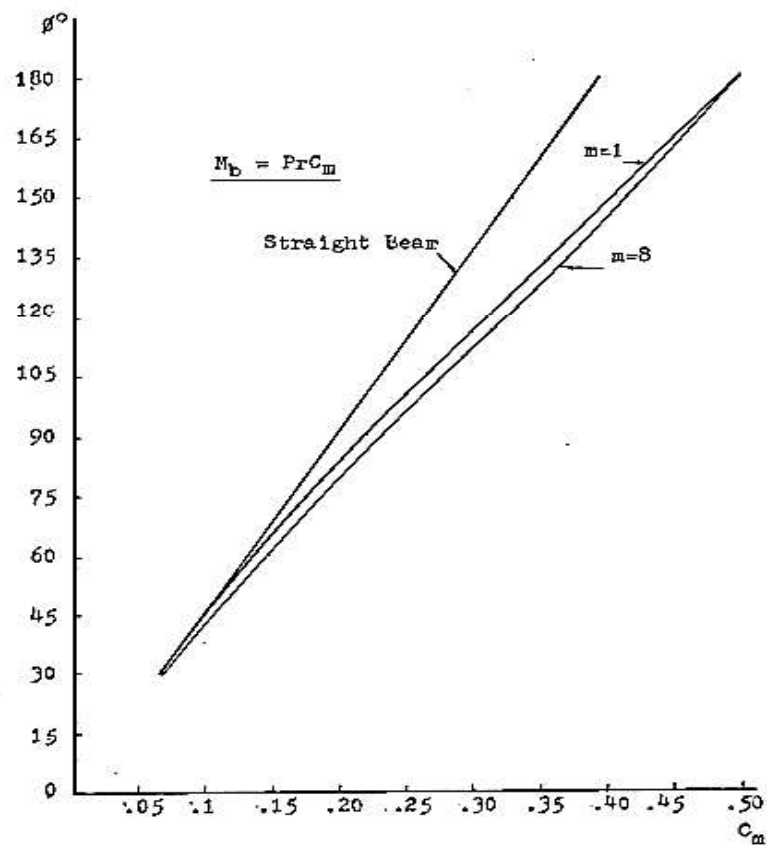


Figure (1-7): Variation of fixed end bending moment coefficients with span angle for horizontally curved beams loaded with concentrated load. (Yee-Chit Wong, 1970)

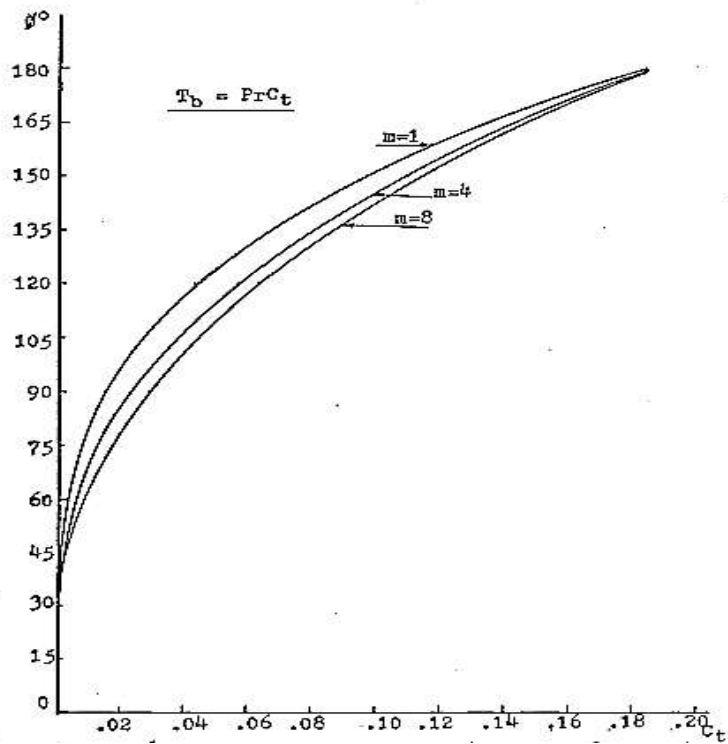


Figure (1-8): Variation of fixed end torsional moment coefficients with span angle for horizontally curved beams loaded with concentrated load. (Yee-Chit Wong, 1970)

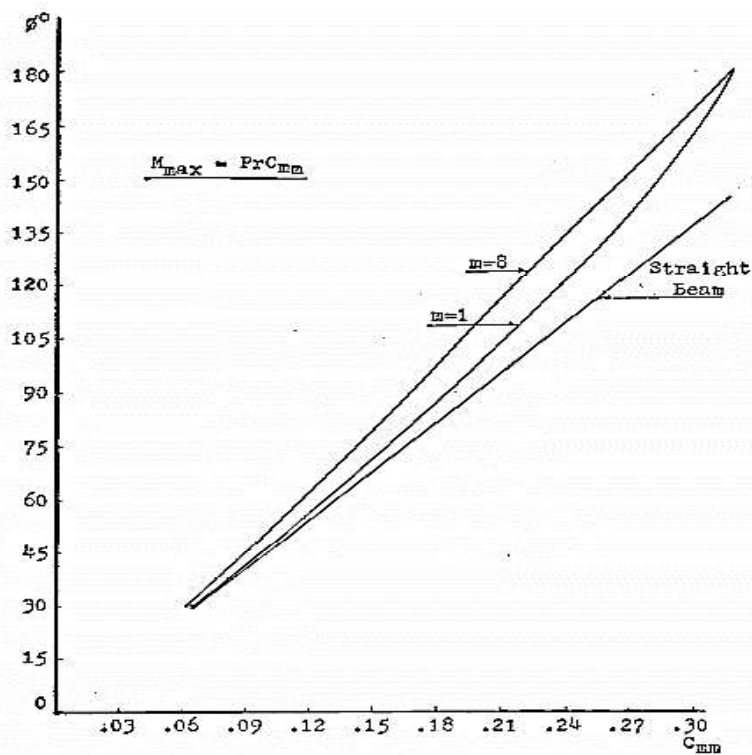


Figure (1-9): Variation of maximum span moment coefficients with span angle for horizontally curved beams loaded with concentrated load. (Yee-Chit Wong, 1970)

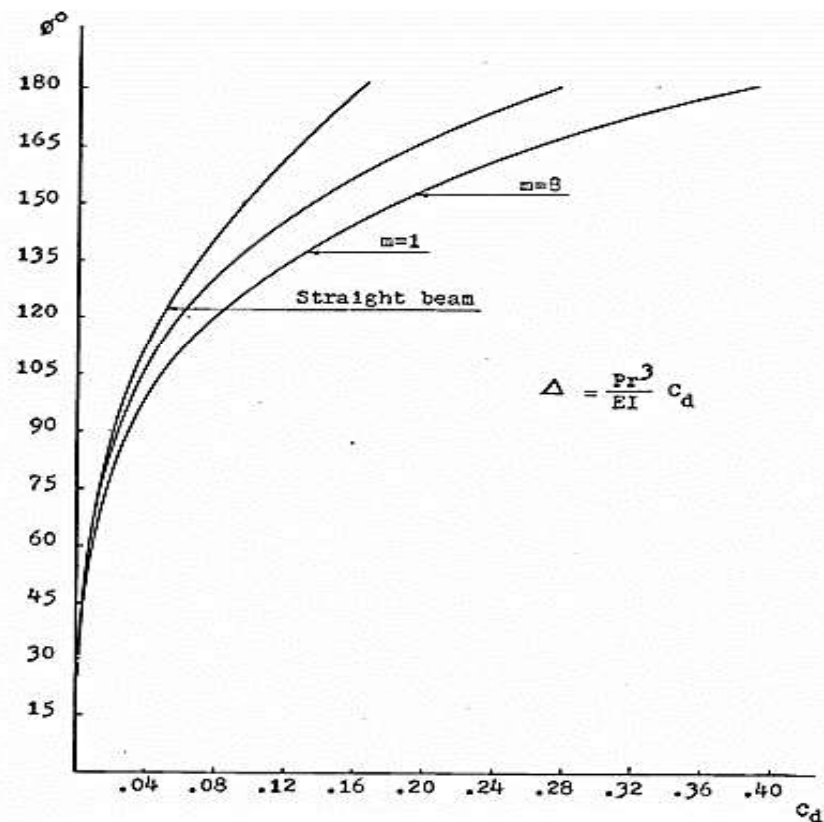


Figure (1-10): Variation of deflection coefficients with span angle for horizontally curved beams loaded with concentrated load. (Yee–Chit Wong, 1970)

Where m depends on the material and shape of the section. It can be calculated in the following manner:

$$m = \frac{EI}{GJ} = \frac{EI}{\frac{E}{2(1+\mu)}J} = \frac{2(1+\mu)I}{J} \quad \text{----- (1-5)}$$

For rectangular section, Figure (1-11),

$$I = bh^3 / 12 \quad \text{----- (1-6)}$$

Where: b and h are the section dimensions of the parallel and perpendicular to the radial axis, respectively.

$$J = 0.33(h - 0.53b)b^3 \quad \text{----- (1-7)}$$

where: h is the long dimension and b is another dimension of the rectangular section.

If the section is so placed that the short side is parallel and the long side is perpendicular to the radial axis, Figure (1-11):

$$m = \frac{(1+\mu)h^3}{2b^2(h-0.63b)} \quad \text{----- (1-8)}$$

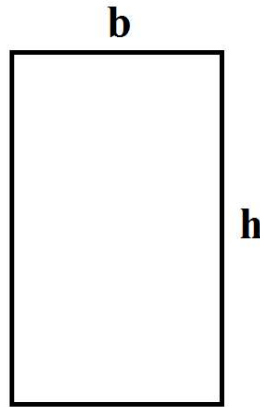


Figure (1-11): Rectangular section of a deep beam

1.4.2 Finite Element Analysis using ETABS 2018

ETABS software is an engineering product that has been used here to analyze the reinforced concrete ring deep beam. ETABS software contains modeling tools and templates, ACI 318 code-based load characterization, analysis method and solution techniques, all coordinate with the grid-like geometry unique to this class of structure, etc... ETABS computerizes the FEA (Finite element Analysis) for predicting how the ring beam reacts to actual final loads. ETABS utilizes the FEA to divide a real reinforced concrete ring deep beam into a large number of finite elements. Mathematical equations help predicting the behavior of each element. Once modeling is completed, ETABS automatically generates and assigns ACI 318 code-based loading conditions for gravity in addition to the applied forces. ETABS software gives the current work a dose of confidence and sobriety to the aforementioned hand calculation analysis.

1.5 Reinforcement limitations

1.5.1 Secondary reinforcement limitations

The secondary reinforcement distribution along with the side faces of deep beams shall be at least as required in (a) and (b) (ACI 318-14, 9.9.3.1):

(a) The “distributed reinforcement area normal to the longitudinal beam axis, A_v , shall be at least $0.0025b_w s$, provided that the spacing of the distributed transverse reinforcement is s ”.

(b) The “distributed reinforcement area parallel to the longitudinal axis of the beam, A_{vh} , shall be at least $0.0025b_w s_2$, where s_2 is the spacing of the longitudinal reinforcement distribution”. The spacing of the necessary distributed reinforcement shall not exceed 300mm and $d/5$ (ACI 318-14, 9.9.4.3).

1.5.2 Main reinforcement limitations

The minimum flexural tension reinforcement area, $A_{s,min}$, is the larger of (a) and (b), for a statically determinate beam (ACI 318-19, 9.9.3.2):

$$(a) \frac{0.25\sqrt{f'c}}{F_y} b_w d \quad \text{----- (1-9)}$$

$$(b) \frac{1.4}{F_y} b_w d \quad \text{----- (1-10)}$$

1.5.3 Concrete cover limitations

Unless a higher concrete cover for fire protection is provided by the general construction code, the minimum defined concrete cover approach is 75 mm maximum and 10 mm minimum (ACI 318-19M, 20.5.1.1).

1.6 Advantages of using the deep ring beams

Ring deep beam are very important structure elements meanwhile, ring beams with full circular in plan are mostly encountered in dome, circular reservoir, silo, offshore structure and others as shown in figure (1-12). The

ring deep beams have been used by industries due to its high loading resistance.



Figure (1-12): Ring beams

1.7 Objectives of the study

The first objective of the current study is experimentally investigating the effect of some important parameters on the behavior of reinforced concrete ring deep beams. The second objective of the current study is to investigate the efficacy of strut and tie method (STM), depending on the fact that the ring beam under study is a deep member. The parameters that are taken into the considerations:

1. Main steel reinforcement,
2. Vertical and horizontal secondary shear steel reinforcements,

3. Height of the reinforced concrete ring deep beam, and
4. Number of supports on which the reinforced concrete ring deep beam rests.

1.8 Thesis Layout

The current thesis consists of five chapters which can be summarized as follows:

- **Chapter One** represents a general introduction about RC deep ring beams, STM, horizontally curved beam, analysis of ring deep beam, reinforcement limitations, in addition to the study objectives.
- **Chapter Two** represents a review of previous research works with experimental investigations that are achieved on reinforced concrete deep ring beams, horizontally curved beams, continuous deep beams and STM validation.
- **Chapter Three** deals with the properties of the utilized construction materials in addition to the experimental work plan.
- **Chapter Four** deals with presenting test results of the laboratory specimens, evaluating and discussing the experimental results of the current study.
- **Chapter Five** provides the main conclusions drawn from the current study, recommendations, and suggestions for further studies.